Experimental study of critical heat flux of refrigerant R1234yf in a multi-minichannel heat sink at medium saturation temperatures

W Imparato[1], R Mastrullo[1], A W Mauro[1,2] and L Viscito[1]

[1]Department of Industrial Engineering, Federico II University of Naples, P.le Tecchio 80, 80125, Naples (Italy)

[2]E-mail: alfonsowilliam.mauro@unina.it

Abstract. The main objective of this work is to present experimental results of saturated flow boiling critical heat flux for refrigerant R1234yf at medium reduced pressures. Tests were carried out by taking into account the influence of the saturation temperature and the mass flux. The former was let to vary from 25 up to 45 °C and the latter ranged from 150 up to 300 kg/m²s. The inlet sub-cooling was set from 6 to 10 K. Results are given in the form of boiling curves, from which the CHF was deduced as the heat flux corresponding to an evident decrease in the curve slope and a sudden spike of the wall superheat. The experimental results have shown that the mass flux has a significant influence on the CHF, whilst the latter is almost independent on the saturation temperature.

1. Introduction

New synthetic refrigerants such as R1234yf represent interesting candidates for the substitution of R134a as operating fluids in refrigerating systems, thanks to a low GWP value and similar thermodynamic properties to other HFCs. The wide spread of micro-electronic devices has risen the scientific interests towards small size cooling elements in which the heat is dissipated through boiling processes of refrigerants at high saturation temperatures, thanks to the great efficiency of the heat transfer.

Moreover, new photovoltaic cells are able to concentrate the solar illumination in small spots, and these systems need to be cooled down in order not to damage the electronic equipment and to maintain the cells efficiency at reasonable values. In this regard, heat sinks made up of micro-channels with boiling refrigerants represent an interesting solution, especially for densely packed cells with very high solar concentration (> 150 suns). For these applications, the heat to be dissipated is beyond the traditional sub-cooled liquid water systems and the fans' air forced convection limits.

In this context, the critical heat flux (CHF) refers to the highest thermal load that can be handled in heat flux controlled devices. Exceeding such limit may lead to a lack of liquid in the heated surface and a subsequent sharp increase in the wall surface temperature, with consequent irreversible failures.

Lazarek and Black [1] performed experimental tests on critical heat flux for R113 in a round tube with an internal diameter of 0.31 cm and with two different heated lengths. A correlation was developed to predict critical conditions under low reduced pressures.

Wojtan et al. [2] investigated different conditions of boiling R134a and R245fa to obtain the saturated critical heat flux in 0.5 and 0.8 mm internal diameter tubes with two different heated lengths. In their results, a strong dependence of CHF on mass velocity, heated length and microchannel diameter was detected. On the contrary, no influence of liquid sub-cooling was observed. Furthermore, a new correlation for the prediction of CHF during saturated boiling in microchannels was proposed by the authors.

Park and Thome [3] tested R134a, R236fa, R245fa CHF in two different multi-microchannels copper heat sinks. CHF was observed to increase when increasing the mass velocity, but the increase rate was slower for higher mass fluxes. CHF was instead seen to decrease with increasing inlet saturation temperature. These trends were found to be dependent both on the flow condition and the channel size.

Mauro et al. [4] studied saturated critical heat flux of R134a, R236fa and R245fa in a multi-microchannel copper heat sink, formed by 29 parallel channels that were 199 μm wide and 756 μm deep. The parametric effects of mass velocity, saturation temperature and inlet sub-cooling were investigated. It was found that higher CHFs were obtainable with a split flow system (by means of one inlet and two outlets), providing also a much lower pressure drop.

Tibiriçá et al. [5] obtained CHF results in circular tubes using R134a and R245fa and compared them against experimental data obtained with flattened tube having the same equivalent internal diameter of 2.2 mm, but different aspect ratios of 1/4, 1/2, 2 and 4. The CHF data were found to be independent on the tube aspect ratio when the same heated length was kept.

Although heat transfer characteristics of different synthetic fluids have already been studied for both conventional and mini-channels, quantitative data of critical heat flux for low-GWP fluorinated refrigerants at medium-to-high saturation temperatures are still limited.

Diani et al. [6]-[7] investigated on flow boiling heat transfer of R1234yf and R1234ze inside a 3.4 mm internal diameter microfin tube. The authors obtained CHF values by keeping constant the inlet vapour quality at 0.3. For both fluids, they found that the critical heat flux, defined as the heat flux on the onset of the dryout condition, was increasing with increasing mass velocity.

Anwar et al. [8] performed several tests with R1234yf in a vertical stainless steel test section (1.60 mm inside diameter and 245 mm heated length) under upward flow conditions. They found that signs of dryout first appeared at vapor qualities of 85%, with the values generally increasing with increasing mass flux.

Anwar et al. [9] reported experimental results on dryout of seven refrigerants (R134a, R1234yf, R152a, R22, R245fa, R290 and R600a) in small, single vertical tubes (0.64–1.70 mm and 213–245 mm heated length) under a variety of operating conditions. The authors found that the dryout heat flux increased with increasing mass flux and with increasing tube diameter. No effect of varying saturation temperature was observed. The experimental findings were compared with well-known macro and micro-scale correlations from the literature and a new correlation for prediction of heat flux at dryout conditions was also developed.

These recent works are mainly related to a single channel geometry, which has the advantage of a feasible control of local parameters (such as the vapor quality along the test section). On the other hand a single channel, differently than a multi-minichannels system, is not the realistic representation of a system able to remove high heat fluxes from squared electronic devices, due to greater heated lengths and the absence of possible mal-distribution and back-flows.

The main objective of this paper is to present experimental results of saturated flow boiling critical heat flux for refrigerant R1234yf at medium reduced pressures in an aluminum multi-minichannel heat sink. Differently from other quoted works, the saturation temperature goes by a wider range (25-45 °C) and the heated length is significantly smaller (25 mm), yielding to very different CHF values. Tests were carried out by taking into account the influence both of the saturation temperature and the mass flux. The latter ranged from 150 up to 300 kg/m²s. Results are given in the dedicated section of this paper in the form of boiling curves and diagrams.

2. Test facility and experimental procedure

All the experiments have been carried-out in a closed refrigerant loop where the inlet conditions in terms of pressure, temperature and mass flux were able to be controlled independently. The experimental set-up is located in the Refrigeration Laboratory at the Dipartimento di Ingegneria Industriale of the Università degli Studi di Napoli "Federico II". A schematic diagram of the test facility is shown in Fig. 1. A brief description of the main and cooling loops, as well as of the test section, are given in the following subsections.

2.1. Main and cooling loops

The black line in Fig. 1 refers to the refrigerant closed loop. A magnetic gear pump, powered by a 0.37 kW electrical motor, pushes the liquid refrigerant towards a Coriolis mass flow meter and then it flows into the test section. The pump may elaborate volumetric flow rates within a range of 1.3-2.5 dm^3/min, passing from 1650 rpm to 3400 rpm. An absolute pressure transducer and a resistance thermometer are inserted just before the inlet of the test section in order to determine the R1234yf inlet conditions. A differential pressure transducer measures the pressure drop occurring in crossing the test section. The refrigerant outlet temperature is then procured thanks to another resistance thermometer placed right outside the aluminum multi-minichannel heat sink. The heated organic fluid passes through a throttling valve utilized to manually adjust the system mass flow rate and pressure. The refrigerant then enters a plate heat exchanger in which it condenses thanks to the cold water coming from the secondary loop and finally it flows into a liquid receiver and a double pipe heat exchanger to obtain a slight sub-cooling, before entering the pump again and closing the loop. The main loop is also equipped with a by-pass circuit right after the circulation pump. With the help of a manually-controlled by-pass valve, it is possible to recirculate a certain fraction of the entire organic fluid stream. In this case, very small mass flow rates into the test section can be achieved.

A thermostatic bath supplies demineralized water to the secondary loop. From the suction pipe, the cooling water flows into the double pipe heat exchanger and then it is pumped into the plate heat exchanger to condense the refrigerant in the main loop. An expansion vessel guarantees the restraint of variations of specific volume.

2.2. Description of the test section

In this work, an aluminum multi-minichannel heat sink has been used as test section. Six fins that are 3 mm high, 1.85 mm wide and spaced 2 mm one another are carved into the main block. A photograph of the aluminum heat exchanger is given in Fig. 2. A cogged cover closes the space between fins and provides seven minichannels, that are 2 mm wide, 1 mm high and 35 mm long. In order to prevent mal-distribution due to excessive discrepancies in pressure drop along the channels, two manifolds are provided for the inlet and the outlet section.

The heat sink is electrically heated from the bottom using AC power supply and a ceramic heater put in a dedicated slot carved underneath the test section. In order to guarantee an appropriate thermal contact, a high performance thermal compound is used. According to the manufacturer, the ceramic element is able to provide heating power of 697 (at 25 °C) over a base area of 2.50x2.50 cm^2, thus obtaining a base heat flux up to 110 W/cm^2. The voltage supply is given by a solid state relay, which can provide up to 400 V. The heat power imposed is measured by means of a wattmeter connected between the heater and the solid state relay. Four resistance thermometers (RTDs) are equidistantly placed in the test section to evaluate the wall temperature along the channels.

The insulation of the test rig has been made with an appropriate layer of synthetic rubber, by paying special attention to the test section. According to the manufacturer, the insulating material guarantees a thermal conductivity less than 0.042 W/m K in the whole range of operating conditions.
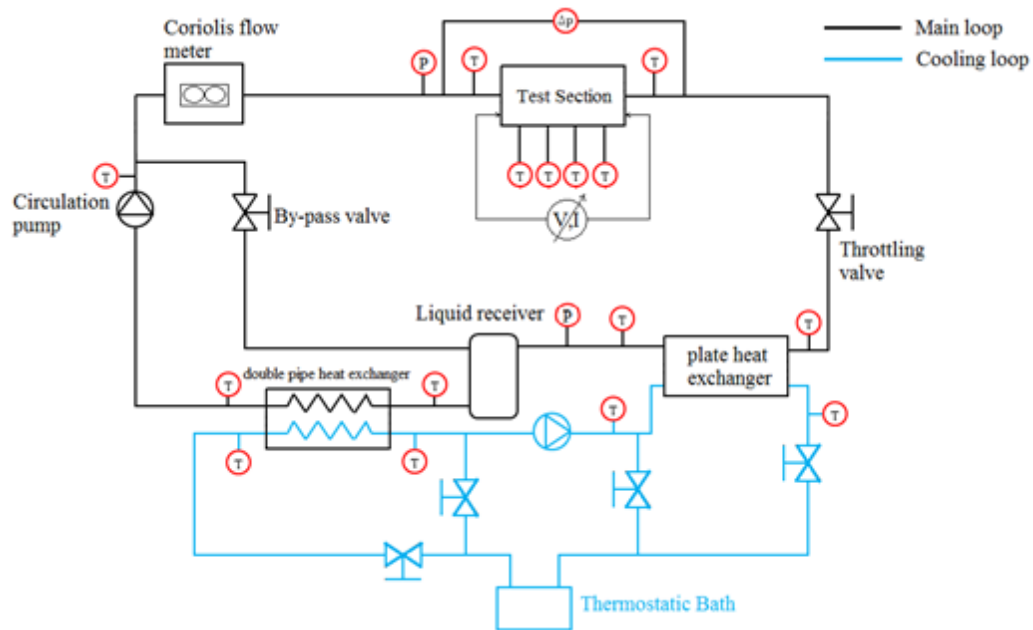
Figure 1 Schematic diagram of the experimental set-up located at the Refrigeration Lab at Università degli Studi di Napoli "Federico II"
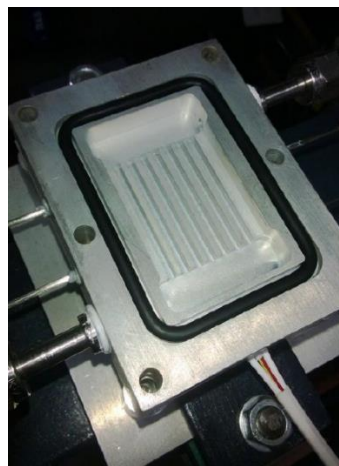

Figure 2 Test section

2.3. Experimental procedure

All tests were performed in steady-state conditions. The desired operating conditions in terms of inlet pressure (i.e. saturation temperature), inlet temperature and mass flux were kept constant at the beginning of each test.

The inlet temperature was manually controlled by opening and closing the secondary loop by-pass valve, thus controlling the cooling water flow into the double pipe heat exchanger. However, the refrigerant mass charge in the test facility was kept reasonably low (2.0 kg) not to have high degrees of sub-cooling in the whole range of saturation temperatures tested.

The remaining parameters were remote-controlled via Labview software and Arduino One controller. Specifically, the system pressure was imposed by setting the temperature of the thermostatic bath, whereas the mass flux was mainly controlled by setting the inverter frequency of the electric motor coupled with the circulation pump. Small adjustments were obtained by manipulating the main loop by-pass valve and by using the throttling valve, thus getting a greater or smaller free flow passage for the refrigerant.

Once the test conditions were set, the heat was applied in small increments by controlling the voltage imposed to the ceramic heater via Arduino One within the range of 0-240 V. The boiling mechanism was then triggered and sustained up to the critical condition. The heater temperature was monitored with a K-type thermocouple and the electrical supply was automatically shut off as soon as the device reached 120 °C, in order not to damage the test section irreparably.

During tests, with increasing imposed heat flux the mass flux was gradually adjusted with the by-pass valve and/or the throttling valve, in order to get the chosen nominal conditions again. The system was considered stabilized when the maximum relative deviation of each value from the measured average in the latest 2 minutes was inferior to 3 %. The recorded time was set to two minutes, with a recording frequency of 1 Hz. Thus, each test was made up of 120 measurements and saved into a text file. The nominal value of each data point was assigned to the sample average value.

The post processing was implemented with the software MATLAB and all the thermodynamic and transport properties were calculated using the software REFPROP 9 [10] developed by NIST.

3. Instrument specifications and uncertainty

The test rig (see Fig. 1) is provided with two absolute pressure transducers. One of them is placed at the inlet of the test section and the other has been put right before the liquid receiver. Both devices measure the absolute pressure within the range 0-50 bar. By taking into account the non-linearity, hysteresis and repeatability effects, the instrument accuracy has a typical value of 0.1 %, with a maximum value of 0.3 % (span error). The resulting uncertainty in absolute pressure measurements is ±0.188 bar.

The pressure drop across the test section is evaluated with the differential pressure transducer Rosemount 2051 within the range of 0-60 kPa. According to the manufacturer, the maximum span error is 0.75 % at full scale, which gives an absolute uncertainty of ±0.45 kPa.

Two resistance thermometers (RTDs) are placed at the inlet and the outlet of the test section, and other identical sensors can be found along the main and the secondary loop (see Fig. 1). Each of them is positioned outside the walls and fixed with a nano-aluminum thermal compound to guarantee the equivalence between the fluid and the measured temperature. According to the manufacturer, all RTDs carry an uncertainty of ±0.180 °C.

Four 4-wire Pt100 cylindrical RTDs are instead positioned along the minichannels for the measure of the wall temperature in the test section. Their uncertainty is found to be ±0.154 °C.

A digital wattmeter is used for the heat power measurements. Its uncertainty results to be 1 %, resulting in a maximum uncertainty of ±10 W at full scale.

The mass flow rate occurring in the test section is measured with a Coriolis flow meter (MicroMotion S12S). The instrument has been tested up to 115.17 g/s and the maximum error was found to be 1 % of the measurement, resulting in an absolute uncertainty of ±1.15 g/s at full scale.

For the calculation of the thermodynamic properties obtained with the software REFPROP 9, it has been considered an uncertainty of 2 %.

Tab.1 summarizes the instrument specifications and their uncertainty, obtained by utilizing a coverage factor of k = 1.

Table 1 Instruments specifications and their uncertainty

Measurement	Range	B type uncertainty (k=1)
Temperature (4-wire Pt100 RTD)	-80 - +250 °C	±0.180 °C
Temperature (4-wire Pt100 cylindrical RTD)	-80 - +250 °C	±0.154 °C
Absolute pressure	0 – 50 bar	±0.188 bar
Differential pressure	0 – 60 kPa	±0.45 kPa
Flow meter	0.00-115.7 g/s	±1 %
Electrical power	0-8 kW	±1 %
Thermodynamic properties (REFPROP software)	-	± 2 %

4. Data reduction

The sensitivity analysis of the CHF results has been performed with respect to the mass flux G and the saturation temperature T_{sat}. The former parameter has been deduced from the measured mass flow rate by taking into account the minichannels cross sectional area:

$$G = \frac{\dot{m}}{N \cdot w_{ch} \cdot h_{ch}} \quad [kg/m^2 s] \tag{1}$$

In the above equation, $\dot{m}$ is the measured mass flow rate [kg/s], whilst N represents the number of minichannels in the aluminum heat sink (N = 7) and w_{ch} and h_{ch} are the minichannels width and height, respectively, expressed in [m].

The saturation temperature, instead, has been evaluated with by knowing the inlet absolute pressure. Since all tests are performed with very low mass fluxes, the measured pressure drop across the test section is insignificant. Therefore, the decrease in the saturation temperature along the minichannels has been considered negligible as well.

The base heat flux supplied from the ceramic heater has been evaluated as:

$$\dot{q}_b = \frac{\dot{Q}}{A_b} \quad [W/cm^2] \tag{2}$$

Where $\dot{Q}$ is the measured heat power and A_b is the heater base area of 2.50 x 2.50 cm^2. The wall heat flux presented in the results section is calculated by taking into account the real heat exchange area, by means of the equation below:

$$\dot{q}_w = \frac{\dot{Q}}{(2 \cdot h_{ch} \cdot \eta + w_{ch}) \cdot N \cdot L_h} \quad [W/cm^2] \tag{3}$$

In the above equation, L_h represents the heated length (L_h = 25 mm) and also the fin efficiency η has been taken into account, following the same approach of Park and Thome [3]. In this work, an average value of η = 0.9 has been chosen.

For the computation of the average wall superheat, the following equation has been considered:

$$\overline{\Delta T}_{wall} = \overline{\overline{T}}_{wall} - T_{sat} \; [°C] \tag{4}$$

The average wall temperature has been calculated with the arithmetical average of the four RTDs placed inside the test section, by neglecting the subtractive term due to the aluminum layer between the RTDs placement and the channels wall.

The inlet R1234yf enthalpy has been evaluated by considering the saturated liquid enthalpy h_l at the inlet pressure and the inlet sub-cooling ΔT_{sub}, whilst the outlet enthalpy follows a simple energy balance:

$$h_{out} = h_{in} + \frac{\dot{Q}}{\dot{m}} \; [kJ/kg] \tag{5}$$

Finally, the vapor quality at the outlet is obtained with the following equation, where Δh_{LV} is the latent heat:

$$x_{out} = \frac{h_{out} - h_l}{\Delta h_{LV}} \tag{6}$$

5. Results

5.1. Adiabaticity tests

41 tests in liquid single phase have been performed in order to verify the correct insulation of the experimental set-up and especially of the test section. The imposed heat has been compared to the heat absorbed by the liquid refrigerant, which results in an increase of its temperature. Fig. 3 shows the injected and the absorbed heat power on the horizontal and vertical axes, respectively. The experimental points' trend is about to be linear and it is compared to the bisector y = x. All the data are very close to the expected values, regardless the heat power injected. In relative terms, the calculated heat loss is significant only for low heat rates, whereas for greater injected heat powers the percentage is reasonably inferior to 4 %. Since all the main tests are performed with higher heat fluxes, the small disruptions in the adiabaticity tests can be neglected.
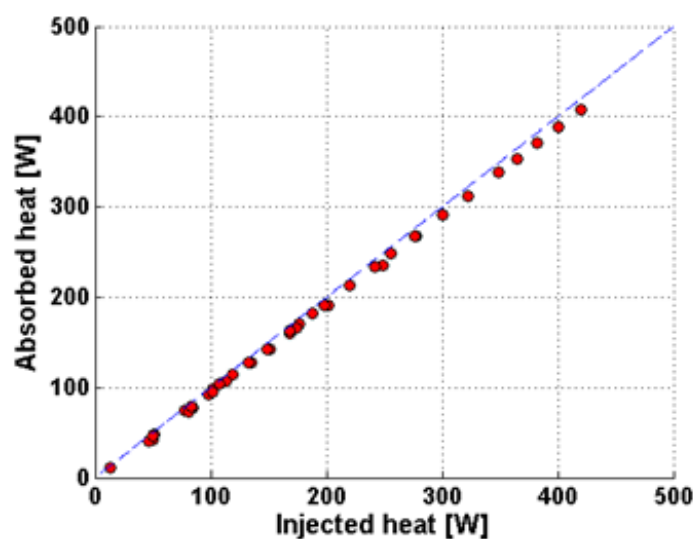

Figure 3 Absorbed versus injected heat power in the test section

5.2. CHF and sensitivity analysis

The main tests have been performed with refrigerant R1234yf at saturation temperatures T_{sat} of 25, 35 and 45 °C, with mass fluxes G ranging from 150 to 300 kg/m^2 s.

The critical condition should be identified when the wall superheat is subjected to a sudden increase with a stable wall heat flux. However, for high mass fluxes, the boiling curves did not exhibit a steep drop in their slope and this behavior has also been observed by Park et al. [3]. In this work the critical heat flux has been defined as the wall heat flux in which the boiling curve decreases its slope $\Delta\dot{q}/\Delta(\Delta T_{wall})$ below a limit value of 2.5 W/cm^2 K, following the same approach of Mauro et al. [4]. Fig. 4 shows two boiling curves obtained in two different operating conditions. The former is taken at a saturation temperature of 25 °C and a mass flux of 148 kg/m^2 s, whereas the latter for a saturation temperature of 35 °C and a mass flux of 250 kg/m^2 s. It is evident that, for the highest mass flux, the thermal crisis is not marked as a sudden flat deviation from the boiling curve trend. This behavior is instead observed for the boiling curve at $G = 148$ kg/m^2 s. The mild decrease in the curves' slope might be due to mal-distribution problems occurring in multi-ducts systems. In a previous study, the test section inlet manifold was provided with an orifice insert which reduced the channels inlet to a 20 % of their original size. This solution was taken in order to apply a consistent pressure drop and thus to prevent possible back-flows. However, even with this configuration, the CHF recorded value did not show significant differences from the present solution and the last part of the boiling curve kept its gentle decrease when obtained at high mass velocities. On the contrary, a higher slope was observed for the first part of the boiling curves at any operating condition, meaning a significant increase in the flow boiling heat transfer coefficient. This was probably explained by a flash evaporation through the orifices which instantly turned the flow pattern into an annular regime. In this regard, the recent work of Tibiriçá et al. [11] showed that an inlet positive vapor quality was able to enhance the CHF if compared to a sub-cooled liquid entry. Yet, the effects of the liquid droplets (entrainment) depletion as well as the inlet vapor quality on CHF has to be further investigated.

The parametric effects of mass flux and saturation temperature have been investigated, whilst the inlet sub-cooling effect was not taken into consideration since it has been seen [3] that, except for very high values (e.g. 20 K), it plays a negligible role in determining the critical condition, especially for macro-scale devices.

The parametric effect of the saturation temperature on CHF is shown in Fig. 5. The first diagram refers to G = 149 kg/m^2 s, whereas the second to a mass flux of G = 300 kg/m^2 s. In both of them, the saturation temperature varies from 25 to 35 °C. The critical condition is considerably higher for the highest mass flux, but the effect of the saturation temperature is almost negligible. In other words, CHFs are the same for the same mass flux and different saturation temperatures, even if the thermal crisis may occur at slightly inferior wall superheat when augmenting the system pressure, meaning that the flow boiling heat transfer coefficient is affected by the saturation temperature.

The effect of mass velocity is shown in Fig. 6, where the two diagrams displayed refer to the saturation temperatures of 25 and 45 °C, respectively. The four boiling curves in each graph are obtained for mass fluxes equal to 148, 200, 250 and 300 kg/m^2 s. CHF increases significantly when increasing the mass velocity at a fixed saturation temperature, whereas the first part of the boiling curves blend one another.

The negligible influence of both mass velocity and average vapor quality on the average heat transfer coefficient might be explained by looking at the similar behavior of the local parameters analyzed by Diani et al. [6] in their 3.4 mm internal diameter single tube.
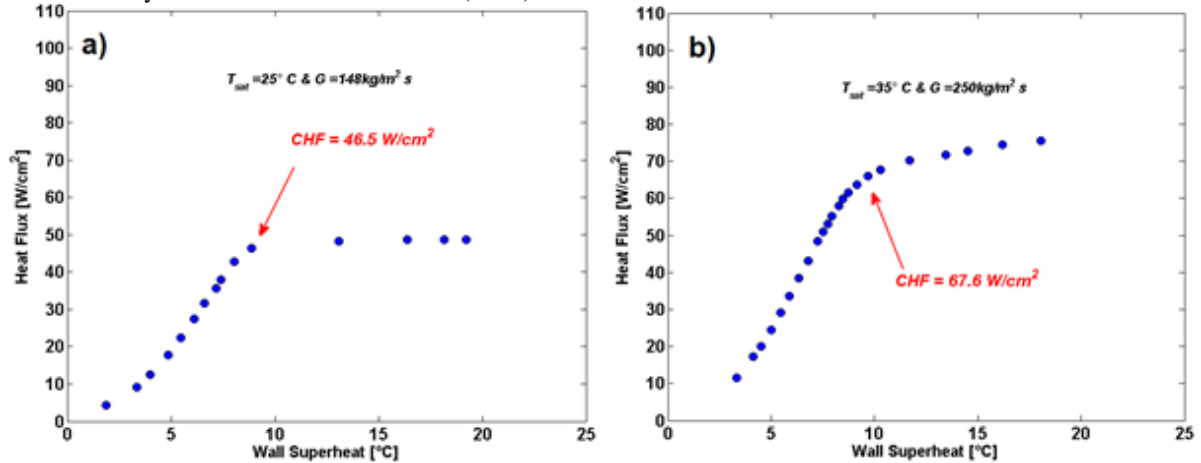
Figure 4 Boiling curves for refrigerant R1234yf at:
a) T_{sat} = 25 °C and G = 148 kg/m^2 s; b) T_{sat} = 35 °C and G = 250 kg/m^2 s
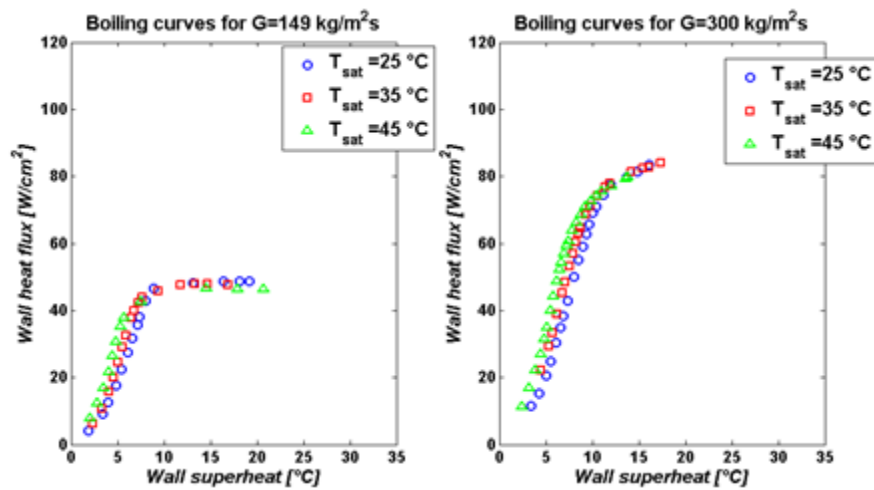

Figure 5 Effect of saturation temperature on CHF for two different mass velocities
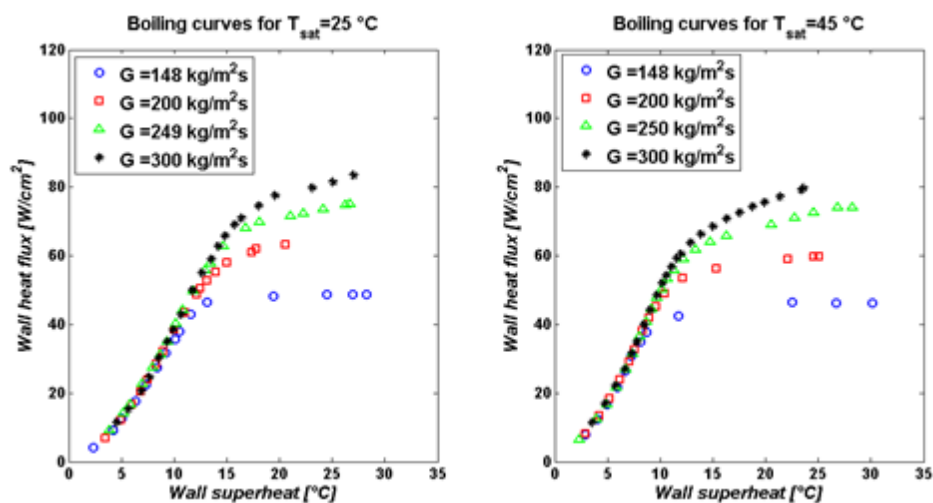

Figure 6 Effect of mass velocity on CHF for two different saturation temperatures
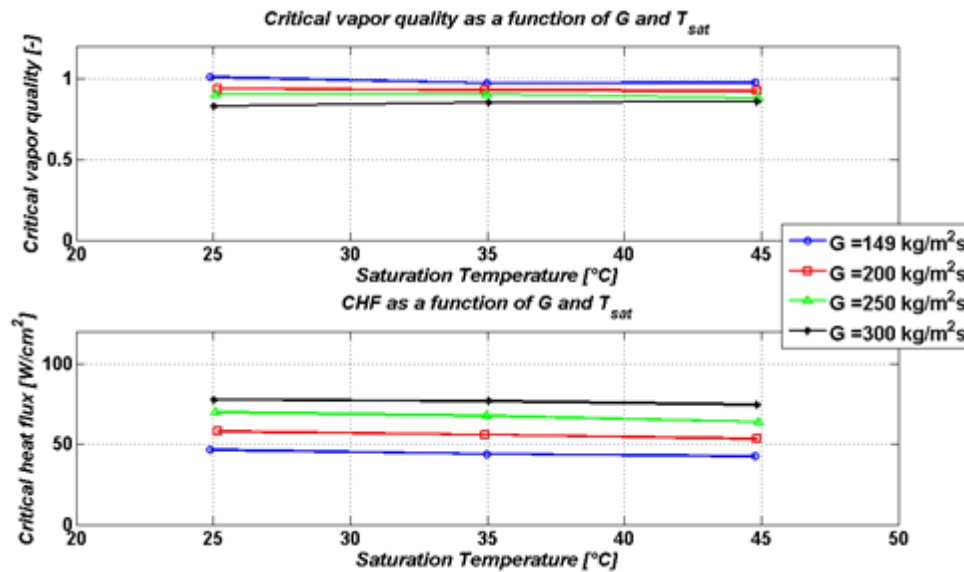
Figure 7 Critical values as a function of the saturation temperature and the mass velocity

Finally, the experimental CHF and critical vapor quality (meaning the outlet vapor quality recorded when the thermal crisis occurred) are plotted in Fig. 7. It is summarized that CHF remarkably increases when increasing mass velocity, whereas for a fixed mass flux it is almost constant within the range of the saturation temperatures investigated. Due to the very small heated length, it is worth noting that experimental CHF values are considerably higher when compared to values obtained in similar studies [8]-[9].

The critical vapor quality does not show a specific trend with the saturation temperature, remaining unchanged from 25 up to 45 °C, at any mass flux displayed. When increasing the mass flux, instead, the critical vapor quality tends to shift towards lower values. Similar results have been obtained in other works available in open literature [2], [3], [8] and [9].

6. Conclusions

Several tests for the investigation of saturated critical heat flux (CHF) of refrigerant R1234yf in a multi-minichannel aluminum heat sink have been proposed in this work. The effect of the mass flux and the system pressure (i.e. the saturation temperature) on CHF and on the boiling curves have been investigated in the range 149-300 kg/m^2 s and 25-45 °C, respectively. The main conclusions are summarized below:

- CHF is significantly affected by the mass flux. When increasing the mass velocity at a fixed saturation temperature, the critical heat flux increases as well.
- The effect of the saturation temperature on CHF is almost negligible. By keeping constant the mass velocity, the thermal crisis occurs approximately at the same heat flux in the range of saturation temperatures investigated, even if a slight decrease is recorded when passing from 25 °C to 45 °C.
- In flow boiling of R1234yf, the average heat transfer coefficient, deduced as the slope in the boiling curves, is moderately affected by the saturation temperature, but when the latter has been fixed it remains almost constant in the whole range of mass velocities investigated.
- The critical vapor quality decreases when increasing the mass flux, whereas it is not affected by a change in the saturation temperature.

However, further studies are required in order to understand the behavior of compact heat sinks handling high thermal loads. More tests at higher mass fluxes and saturation temperatures are needed, as well as a comparison between CHF of different low GWP refrigerants. Finally, experimental CHF values of new refrigerants have to be compared with well-known correlations available in scientific literature.

References

[1]   Lazarek G M and Black S H 1982 Evaporative heat transfer, pressure drop and critical heat flux in a small vertical tube with R-113 *Int. J. of Heat and Mass Transfer* **25** 945-960.

[2]   Wojtan L, Revellin R and Thome J R 2006 Invetigation of saturated critical heat flux in a single, uniformly heated microchannel *Experimental Thermal and Fluid Science* **30** 765-774.

[3]   Park J E and Thome J R 2010 Critical heat flux in multi-microchannel copper elements with low pressure refrigerants *Int. J. of Heat and Mass Transfer* **53** 110-122.

[4]   Mauro A W, Thome J R, Toto D and Vanoli G P 2010 Saturated critical heat flux in a multi-microchannel heat sink fed by a split flow system *Experimental Thermal and Fluid Science* **34** 81-92

[5]   Tibiriçá C, Ribatski G and Thome J R 2012 Saturated flow boiling heat transfer and critical heat flux in small horizontal flattened tubes *Int. J. of Heat and Mass Transfer* **55**, 7873-7883.

[6]   Diani A, Mancin S and Rossetto L 2015 Flow boiling heat transfer of R1234yf inside a 3.4 mm ID microfin tube *Experimental Thermal and fluid Science* **66** 127-136.

[7]   Diani A, Mancin S and Rossetto L 2015 Flow boiling heat transfer of R1234ze(E) inside a 3.4 mm ID microfin tube 2014 *Int. J. of Refrigeration* **47** 105-119.

[8]   Anwar Z, Palm B and Khodabandeh R 2015 Flow boiling heat transfer, pressure drop and dryout characteristics of R1234yf: Experimental results and predictions *Experimental Thermal and fluid Science* **66** 137-149.

[9]   Anwar Z, Palm B and Khodabandeh R 2015 Dryout characteristics of natural and synthetic refrigerants in single vertical mini-channels *Experimental Thermal and fluid Science* **68** 257-267.

[10]   Lemmon E W, Mc Linden M O and Huber M L 2009 REFPROP *NIST Standard Reference Database* **23***, Version 9.0.*

[11]   Tibiriçá C, Czelusniak L E and Ribatski G 2015 Critical heat flux in a 0.38 mm microchannel and actions for suppressing of flow boiling instabilities *Experimental Thermal and Fluid Science* – Article in press.